UCRL-JC-129774
PREPRINT

Measurements of Near Forward Scattered Laser Light in a Large ICF Plasma

J. D. Moody, B. J. MacGowan, B. B. Afeyan, S. H. Glenzer, R. K. Kirkwood, S. M. Pollaine, A. J. Schmitt, E. A. Williams

This paper was prepared for submittal to the
12th Topical Conference on High-Temperature Plasma Diagnostics
Princeton, NJ
June 7-11, 1998

June 2, 1998

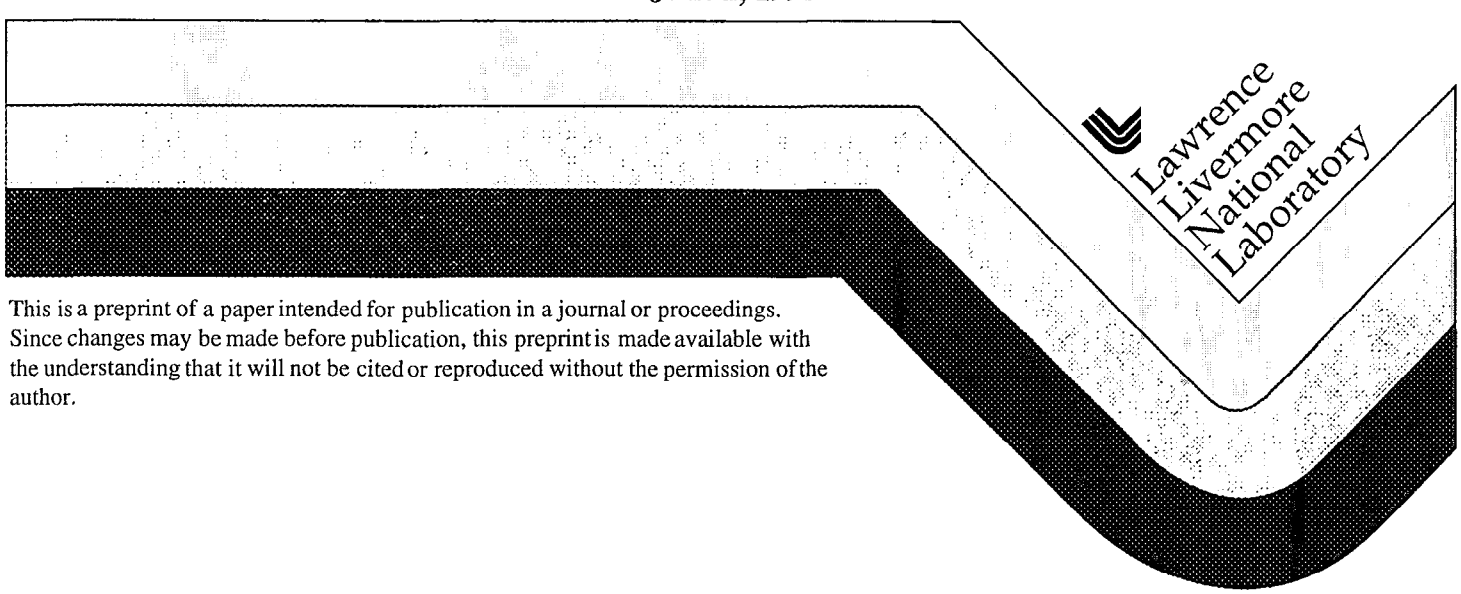

Measurements of near forward scattered laser light in a large ICF plasma

J. D. Moody, B. J. MacGowan, B. B. Afeyan, S. H. Glenzer,
R. K. Kirkwood, S. M. Pollaine, A. J. Schmitt, and E. A. Williams
Lawrence Livermore National Laboratory
University of California
Livermore, CA 94551

Abstract

We describe an instrument which measures the angular spread and spectrum of near forward scattered laser light from a probe beam in a long scalelength laser-plasma. The instrument consists of a combination of time integrating and time resolving detectors which measure the scattered light amplitude over four orders of magnitude for a range of angles. These measurements allow us to study the beam spray resulting from various laser and plasma conditions and determine the density fluctuations associated with this beam spray.

I. Introduction

The laser intensity and spot characteristics on the wall of an indirect drive gas filled hohlraum[1]determine the temperature and symmetry of radiation on the fuel capsule. As a result, phenomena which affect the propagation of laser energy through the hohlraum gas plasma are important to inertial confinement fusion (ICF). Effects such as inverse bremmstrahlung absorption, stimulated scattering, filamentation, beam deflection, and beam spray in the hohlraum gas plasma can both attenuate the incident laser light as well as spread and shift the laser spot location on the hohlraum wall. It is important to understand these effects in order to account for them in the design of future NIF ignition targets.

A correct understanding of the laser propagation through the hohlraum gas plasma relies on the ability to make detailed optical measurements. We can accomplish this by studying laser propagation in an open geometry target designed to have similar gas plasma characteristics as the hohlraum gas plasma. This target, called a gasbag, resembles the hohlraum gas plasma in density, temperature, and scalelength and provides open access for measuring scattered and transmitted optical light. As a result, back, side, and forward scattered light can be measured and a detailed analysis of laser propagation, beam spray, and beam deflection in this target can be caried out.

This paper describes an instrument used to obtain detailed measurements of the forward scattered light from a probe laser which is incident on a gasbag plasma. The instrument detects the angle-dependent scattered light amplitude and the spectral character of this light. We are interested in these measurements primarily for two reasons. First, they indicate the severety of beam spray due to the laser propagation through the gas plasma. This spray changes the relative amplitudes of the spherical harmonics describing the x-ray illumination of a hohlraum capsule. As a result, beam spray is more difficult to correct than beam deflection for example. Correcting the asymmetry resulting from beam spray requires adjusting the relative

power distributed in the beams. Asymmetries introduced by beam deflection can be corrected by static or dynamic pointing changes. In addition to beam spray we would like to determine quantitatively the density fluctuations in the gas plasma. These fluctuations can affect the laser-plasma instabilities which produce backscattered light and we are interested in determining what role the fluctuations have in suppressing or enhancing the backscattering. The instrument that we will describe can detect fluctuations with scalelengths less than about 7μm. The remainder of the paper describes the forward scattered light instrument, gives examples of the measurements, and presents an interpretation of the data.

II. Gasbag target

The experiments were conducted on the Nova laser facility at the Lawrence Livermore National Laboratory. This is a ten beam Nd:glass laser system typically operating at third harmonic (351 nm). The gas balloon target[2] consists of two circular polyimide membranes attached to the sides of an Al washer. The space between the membranes is pressurized to about 1 atm with C_5H_{12} gas. Nine of the beams heat the target with a total of 21 to 25 kJ at nearly constant power for 1 ns at an intensity of about $1.5 \times 10^{14}\,\mathrm{W/cm^2}$. Laser heating of the target has been extensively characterized with x-ray measurements[3] which show that T_e becomes uniform after about 0.3 ns and steadily rises to about 2.5 keV. The probe beam has a variable intensity ranging from about $1 \times 10^{15}\,\mathrm{W/cm^2}$ to $2 \times 10^{16}\,\mathrm{W/cm^2}$ and is smoothed with an RPP[4-5] phase plate giving a speckle distribution of intensities in a focal spot of about 220μm FWHM. The probe is focused to the target center with an f/4.3 optic, turns on 0.4 ns after the heater beams, and lasts for 1 ns.

III. The forward scattered light instrument

The forward scattered light instrument consists of two different sensitivity detectors which together can measure light levels over about 4 orders of magnitude. Figure 1 (a) shows a schematic of the forward scatter instrument and Fig. 1 (b)

shows a picture of the instrument as viewed along the propagation direction of the probe beam. The majority of the forward directed light transmitted through the target remains within the incident f/4.3 cone and is measured with the low sensitivity detector. This detector consists of a large frosted silica scatter plate (extends to f/2 angular coverage) which diffusely scatters the transmitted light with an angular distribution peaked in the direction normal to the scatter plate. This part of the transmitted light instrument has been described in Ref. [6]. The diffusely scattered light intensity is proportional to the incident light intensity and is measured with a fast photodiode and a gated optical imager (GOI). The diode gives the time-dependent power on the plate and the GOI records the angular power distribution on the plate at three different gate times evenly spaced throughout the probe pulse.

The flux of light which scatters outside of the main f/4.3 beam cone rapidly decreases in amplitude with increasing angle. Detecting this signal requires much more sensitivity than is possible with the scatter plate so we use a technique which employes direct optical detection of this light. Ten or more detectors, placed at angles ranging from 8° to 35° from the forward direction, collect a sample of the light scattered at these angles. The detectors are half-inch concave silica substrates with a 1.5 m radius of curvature. The detectors near to the f/4.3 cone angle are uncoated and reflect about 4% of the light striking the substrate. Detectors further out in forward angle are aluminized so that about 90% of the light reaching these detectors is reflected. The reflected light is directed through a BK7 glass target chamber port to instruments outside of the chamber. As the light propagates across the target chamber between the detector and the port it passes through a focus and expands to a diameter of about 1.5 cm at the location of the chamber port. After exiting the chamber the light is imaged by a 75 mm diameter lens onto a Spectralon diffuser plate. The lens forms a demagnified image of the detectors showing the brightness level of light reflected by each of the 1/2 inch mirrors. The signals imaged onto the diffuser plate are viewed by two 8-bit CCD cameras filtered differently by about a

factor of 5 in order to give a wider dynamic range for the measured signal. Both cameras additionally use a bandpass filter having a pass band of 10 nm centered at 355 nm. This is used to block any unconverted laser light or forward Raman light which may contaminate the forward scattered light signal near 351 nm.

The mirror detection system has several advantages over other techniques which use photosensitive electrical devices such as photodiodes and calorimeters. The electromagnetic pulse during a target shot can introduce noise on electrical cables attached to electrical detectors inside of the target chamber; the mirror detectors are not succeptible to this. In addition, the calibration of the electrical detectors must be routinely measured whereas the mirror detectors are constructed to be equivalent (measurements confirm this) and therefore have the same relative sensitivity. Finally, the filtering of the mirror detector signals is done outside the target chamber rather than inside which is the case for electrical detectors. This means that filtration of the mirror signals can be adjusted easily and without venting the target chamber.

In addition to the mirror detectors, six optical fibers are placed at angles ranging from 3° to 25° which measure the spectrum of the forward scattered light. Two of these fibers are located within the f/4.3 cone angle (behind the main scatter plate) and the other 4 are placed at increasing angles from forward. The fibers transport light to a 1 m Czerney-Turner spectrometer coupled to a streak camera. The streak shows the temporal evolution of the high resolution spectrum of light at the different forward angles.

IV. The time-integrated mirror detectors

The uncoated mirrors at small forward angles are orientated so that the incident light direction is about 22° from the mirror surface normal. This gives a reflected signal which is about 1/34 of the incident for P-polarized light and about 1/22 for S-polarized light. The scattered light which reaches these mirrors is roughly

mixed S and P polarization (due to the geometry of the detectors) so that the reflected signal has an amplitude of about 1/27 of the level of light incident on the uncoated mirror. The silvered detectors have a UV protected aluminum coating on the surface giving a reflectivity of 90%. This gives a sensitivity of the silvered detectors which is about 25 times higher than the bare glass detectors. As the forward scattering angle increases the effective area of the aluminized mirrors decreases slightly so that for the one detector at 34° the effective area for collecting scattered light from the target is reduced by about 20%. Finally, a small fraction of the light exiting the chamber through the port is lost due to reflection off of the bare glass port. There are slight variations (10% or less) in this light-loss for the different angularly located detectors. This effect and the slight decrease in detector area with increasing forward angle are small so we neglect corrections to the data which would result from considering them.

The mirror detectors are protected with debris shields to keep ablated target material from coating the mirror surface. These shields are made of 1/16 inch silica and are routinely replaced with clean shields before a series of experiments utilizing the forward scatter instrument. Alignment of the mirror detectors is done using a fiber placed at target chamber center. A 30 mW He-Ne laser is connected to the fiber to give a bright diverging source of light originating from the target location. The optical characteristics of the mirror detectors do not depend on light wavelength (due to reflective optics) so alignment can be done at this convenient wavelength. The detectors are adjusted to direct the reflected portion of light through the chamber port and through the center of the 75 mm focusing optic outside of the chamber. The large 75 mm focusing optic allows for slight shifts in the alignment during pumpdown and eases the mirror alignment tolerances.

Figure 2 shows examples of the data obtained with the mirror detectors. The signal from a gasbg experiment at $n_e/n_{\rm cr} = 0.1$ is shown in Fig. 2 (a) and Fig. 2 (b) shows the signal for an experiment with $n_e/n_{\rm cr} = 0.07$. Detectors at another

azimuthal angle have been added recently and show that the forward scattering is the same at these two angles.

V. The temporally and spectrally resolving fiber detectors

The time dependent behavior of the forward scattered light is determined from the forward scattered light streaks. Figure 3 shows an example of the streaks from two interaction experiments. Each data-record shows 6 streaks. The two within the beam cone show the time history of the transmitted light and indicate a spectrum which is slightly broadened toward the red of the incident 351 nm wavelength. Experiments over a range of intensities show that the broadening increases with probe intensity. The remaining four fiber streaks show two features. The streak begins with sidescattered light from the heater beams which is about 5Å wide and lasts about 0.2 to 0.3 ns. Following this, forward scattered light from the probe appears at about 0.4 ns after the heater beam signal and continues for some time ranging between 0.6 and 1 ns. The duration of the signal is shorter for the detectors at larger forward angles indicating that the beam spray is initially wide and then narrows during the interaction pulse. The four larger angle streaks are also red shifted and broadened. The red shift is in agreement with the classical SBFS red shift at low probe intensities (2×10^{15} W/cm^2) but shows an enhanced red shift at higher intensities. We have considered various explanations to this enhanced red shift such as probe-plasma heating, self phase modulation, and strongly driven SBFS. We find, based on additional measurements and estimates that the most likely explanation is strongly driven SBFS. The broadening can be due to filamentation, plasma induced spectral broadening, damping of the ion acoustic wave participating in SBFS, and scattering from fluctuations. We do not yet know the relative importance of each of these effects.

VI. Instrument calibration

The mirrors and fibers cannot be calibrated in-situ since there are no laser beams which can be pointed directly onto the detectors. As a result, we use a

method which approximately calibrates the detectors. This method uses signals from all three instruments measuring the forward scattered light: the GOI imager, the fiber signals, and the mirror signals. The nearly isotropic 351 nm light which scatters from a gasbag target during the first 0.2 to 0.3 ns of target heating is detected by the fibers as a broadband signal at the beginning of the 4 larger angle streaks shown in Fig. 3. This light is due to scattering from the skin of the gasbag which blows down to below critical density after about 0.2 to 0.3 ns. We have measured this scattered flux to be about 25 J/sr (with a factor of 2 uncertainty) using a series of diode and fiber detectors placed at various angles around the target chamber. This flux corresponds to an average scattering level of 7% during the first 0.2 ns of heating. The first step in the calibration procedure is to calibrate the signal from each of the four fiber detectors according to the initial (25 J/sr) signal from the heater beams. Second, the mirror detectors near the location of the fiber detectors are calibrated so as to agree with the time integrated fiber signals. The remaining mirror detectors are calibrated with the same calibration of the other mirrors since the mirror detectors are essentially equivalent. Third, the one or two large-angle mirror detectors typically have signal which is due only to the heater beam scattered light since the forward scattered light at large angles from the probe beam is small compared to this. The calibrated mirror signal is checked to give about 25 J/sr adding further confirmation that the calibration done using the fiber signals is correct. Finally, one further check of the mirror and fiber calibration is made by comparing the signal on the small angle mirror detectors with the signal measured by the GOI instrument at angles where the two instruments overlap ($6° \leq \theta \leq 15°$). The GOI sensitivity is set so that the bright region of the scatter plate is near detector saturation. This results in a noise level which is about 2% of the bright signal. Most data obtained with the mirror detectors shows a calibrated flux of light at an angle corresponding to the outer portion of the scatter plate of about 1% to 3% of the flux in the central section of the plate. The signal on the GOI image in the range of $6° \leq \theta \leq 15°$ is just reaching the instrument noise level (2% to 4%

of the central scatter plate signal) at the angle where the first mirror detector is located. Thus, the GOI image shows a signal which does not contradict the mirror detectors although it is difficult to say whether the GOI image shows a light flux signal just at the noise level or somewhat below it. Recent f/8 data, where we find more light illuminating the scatter plate at larger angles validates this calibration to within a factor of 3.

VII. Experimental results

Figure 2 (c) shows a line plot of the mirror data after the background has been subtracted and the signals calibrated to correspond to $J_{\rm scat}/sr/J_{\rm inc}$ where $J_{\rm scat}$ is the scattered laser energy and $J_{\rm inc}$ is the incident laser energy. The decrease with angle at both densities is clear from this figure although the shape of the angular fall-off is different indicating a different correlation length of the fluctuations in both cases. Angular spray of several times this level will prevent ignition of a NIF capsule. However, simulations show that readjustment of the power distribution in the beams restores ignition.

We have performed several experiments to determine the level of forward SRS light present in the forward scattered energy. This is done by changing the 351 nm bandpass filter in front of the detector cameras to a different wavelength range. Estimates of this wavelength range for forward SRS light indicate that it ranges between 500 nm and 530 nm. We used a cut-on filter at 500 nm and a cut-off filter at 550 nm to limit the spectral range. The level of SRFS is determined from several interaction experiments to be less than 0.002 J/sr.

VIII. Interpretation of the data

The interpretation of the forward scattering data has been discussed elsewhere (Ref. 7) but we would like to summarize it here. We use the forward scattered amplitude to infer the density fluctuation spectrum which gives the measured angular spread in the forward scattered light. We accomplish this by prescribing the form

of the plasma density fluctuation (PDF) spectrum and computing the resulting angular distribution of scattered light. Matching the observed data by adjusting the PDF spectrum allows us to infer some of its properties. We model this scattering with a wave kinetic equation check with an analytical estimate.

The observed scattered light distribution [Fig. 2 (c)] has a rapid reduction of intensity outside the beam cone down to a broader shoulder of scattered light. We find that this shape can only result if the dominant scattering is not small-angle (compared to the beam cone-angle). Small-angle scattering gives rise to a gradual fall-off of the scattered intensity outside the beam cone. The angular width of the shoulder implies a PDF spectrum with a transverse correlation length of $l_\perp = 4\lambda_0$ at the lowest intensity ($1.5 \times 10^{15}\,\mathrm{W/cm^2}$) and $1.5\lambda_0$ at the higher intensities. It appears that the transverse PDF spectrum is the same as that of the resulting density perturbation impressed by the speckle pattern of the f/4.3 optics at low intensity. This spectrum spreads (by growth of SBFS) to smaller wavelength as the intensity increases.

IX. Summary and future plans

In summary, we have described an instrument which we use to measure the amplitude and spectra of forward scattered light produced from a high intensity smoothed probe beam interacting with a sub-critical long scalelength plasma. We find that classical or strongly driven SBFS causes the majority of near forward scattered light. The small amount of plasma-induced spectral broadening may result from a combination of filamentation, scattering from density inhomogeneities, and damping of the SBFS. An incoherent scattering model reproduces the measured angular spread for a transverse fluctuation spectrum having $< |\delta n/n| >= 0.03$ to 0.005 and a correlation length of 1.5 to 4 probe wavelengths.

Our future plans are to measure the forward scattered light resulting from the Nova 4ω probe laser to determine the level and spectrum of the background

fluctuations. This probe laser is low intensity so that it does not drive any instabilities itself. As a result it passively scatters off of the fluctuations already present in the plasma. The probe is an f/20 beam so that fluctuations with a scalelength as long as 15μm can be detected. Initial measurements using this indicate that the fluctuation level is about $< |\delta n/n| > \sim 10^{-3}$.

The author gratefully acknowledges helpful discussions with A. M. Rubenchik and the help of R. Griffith with the streak camera instrument. This work is performed under the auspices of the U. S. Department of Energy by the Lawrence Livermore National Laboratory under Contract No. W-7405-ENG-48.

REFERENCES

1. J. Lindl, *Phys. of Plasmas* **2**, 3933 (1995).
2. D. H. Kalantar, D. E. Klem, B. J. MacGowan, J. D. Moody, D. S. Montgomery, D. H. Munro, T. D. Shepard, and G. F. Stone, *Phys. Plasmas* **2**, 3161 (1995).
3. S. H. Glenzer, C. A. Back, K. G. Estabrook, B. J. MacGowan, D. S. Montgomery, R. K. Kirkwood, J. D. Moody, D. H. Munro, and G. F. Stone, *Phys. Rev. E* **55**, 927 (1997).
4. S. N. Dixit, I. M. Thomas, B. W. Woods, A. J. Morgan, M. A. Henesian, P. J. Wegner, and H. T. Powell, *Appl. Opt.* **32**, 2543 (1993); J. W. Goodman, *Statistical Optics (Wiley, New York, 1985).*
5. S. Skupsky, R. W. Short, T. Kessler, R. S. Craxton, S. Letzring, and J. M. Soures, *J. Appl. Phys.* **66**, 3456 (1989).
6. J. D. Moody, B. J. MacGowan, R. K. Kirkwood, and D. S. Montgomery, *Review of Scientific Inst.* **68**, 1725 (1997).
7. J. D. Moody, B. J. MacGowan, B. B. Afeyan, S. H. Glenzer, R. K. Kirkwood, W. L. Kruer, D. S. Montgomery, A. J. Schmitt, E. A. Williams, and G. F. Stone, Submitted to *Phys. Rev. Lett.* Feb. 1998.

FIGURE CAPTIONS

FIG. 1 (a) Schematic of forward scattered light instrument. (b) Photograph of the forward scattered light instrument as seen in the Nova target chamber when viewed along the direction of the probe beam.

FIG. 2 (a) Data obtained using the time-integrating mirror detectors for a gasbag plasma with $n_e/n_{\rm cr} = 0.1$ and a probe intensity of $8 \times 10^{15}\,{\rm W/cm^2}$. (b) Mirror detector data for a gasbag plasma with $n_e/n_{\rm cr} = 0.07$ and a probe intensity of $8 \times 10^{15}\,{\rm W/cm^2}$. (c) Line plot showing the angular dependence of the calibrated forward scattered light for the two plasma densities.

FIG. 3 Time resolved streak measurement for (a) low density ($n_e/n_{\rm cr} = 0.07$) gasbag plasma with a probe intensity of $8 \times 10^{15}\,{\rm W/cm^2}$, and (b) high density ($n_e/n_{\rm cr} = 0.1$) gasbag plasma with a probe intensity of $8 \times 10^{15}\,{\rm W/cm^2}$.

Figure 1 (a)

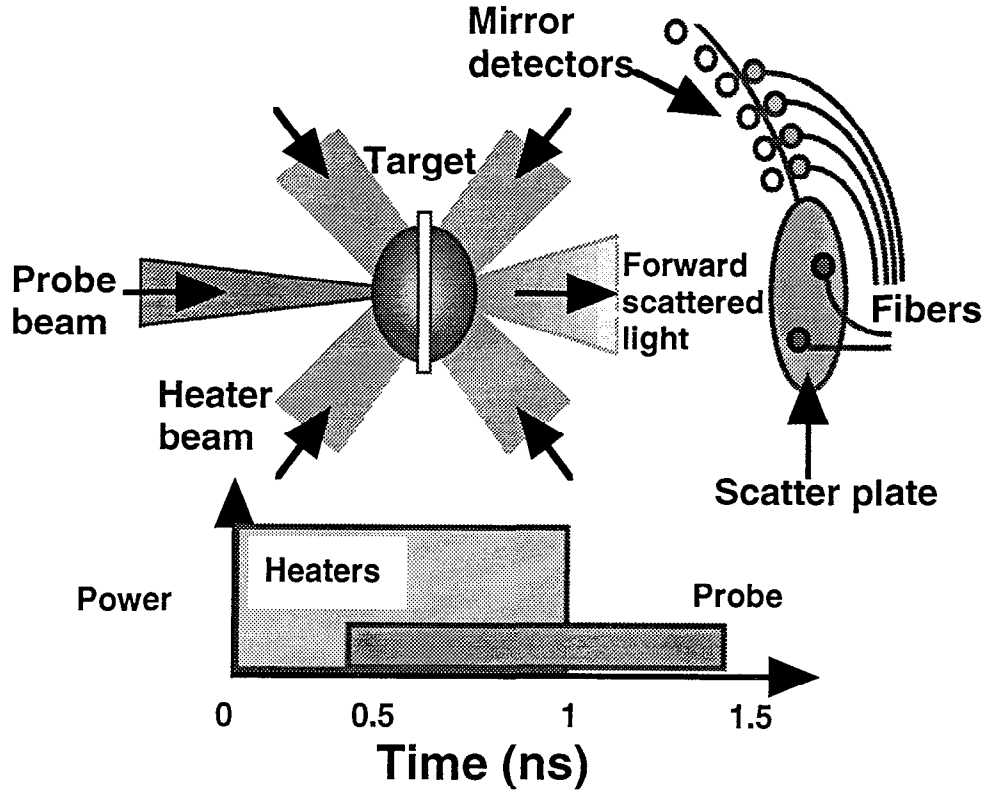
Mirror
detectors
Target
Probe
beam
Forward
scattered
light
Fibers
Heater
beam
Scatter plate
Heaters
Power
Probe
0
0.5
1
1.5
Time (ns)

Figure 1 (b)

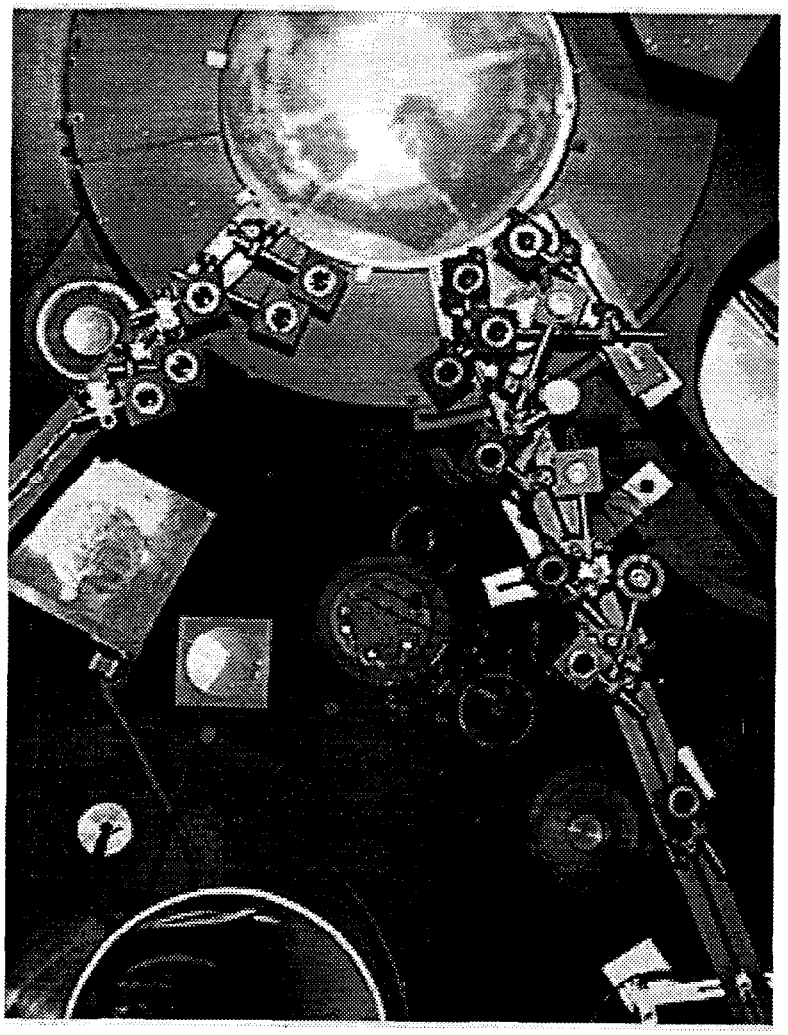

Figure 2

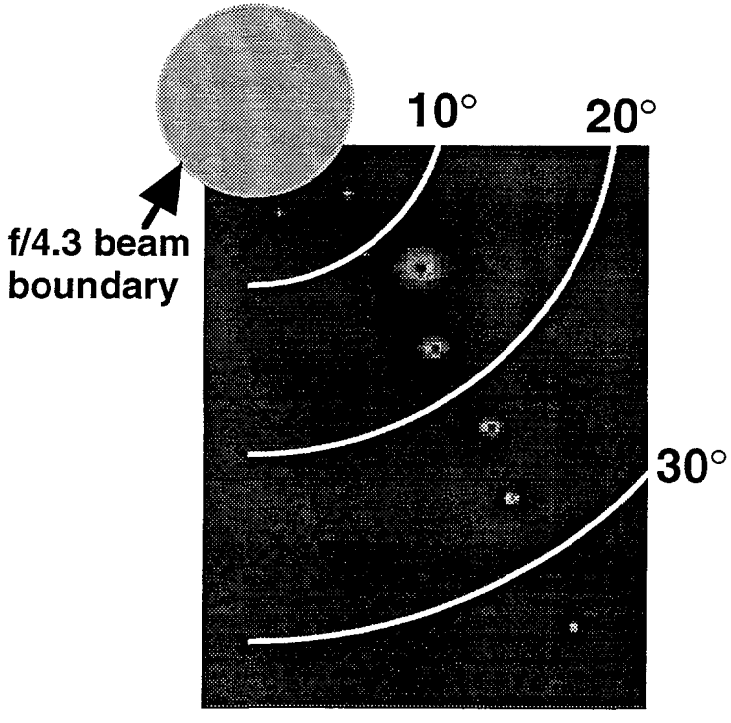

(a)

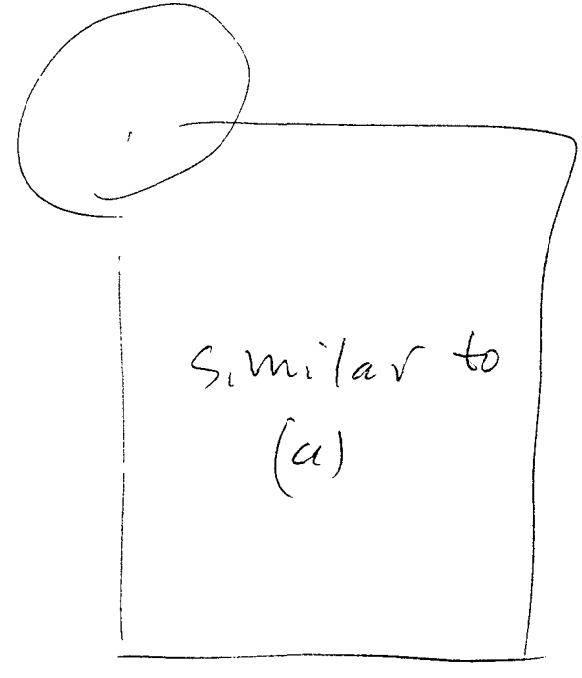

(b)

Figure 2 (c)

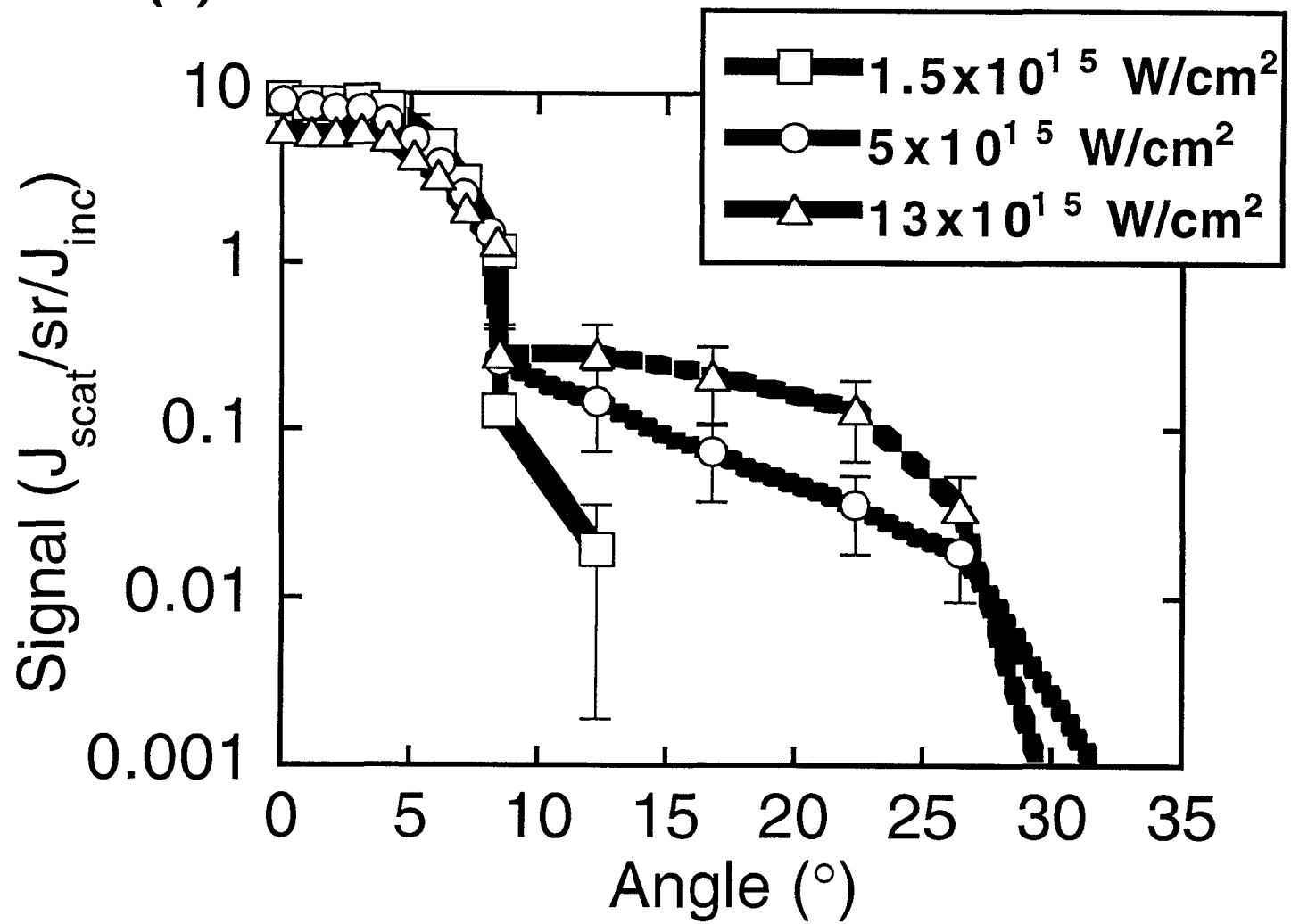
1.5x10^15 W/cm^2
5x10^15 W/cm^2
13x10^15 W/cm^2
Signal (J_scat/sr/J_inc)
10
1
0.1
0.01
0.001
0
5
10
15
20
25
30
35
Angle (°)

Figure 3

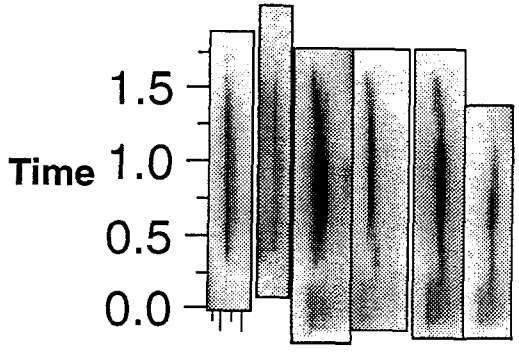

(a)

Similar to (a)

(b)

Technical Information Department • **Lawrence Livermore National Laboratory**
University of California • Livermore, California 94551